SOLVING MIXED DIELECTRIC/CONDUCTING SCATTERING PROBLEM USING ADAPTIVE INTEGRAL METHOD

W.-B. Ewe, L.-W. Li [†], and M.-S. Leong

Department of Electrical and Computer Engineering
National University of Singapore
Kent Ridge, Singapore 119260

Abstract—This paper presents the adaptive integral method (AIM) utilized to solve scattering problem of mixed dielectric/conducting objects. The scattering problem is formulated using the Poggio-Miller-Chang-Harrington-Wu-Tsai (PMCHWT) formulation and the electric field integral equation approach for the dielectric and conducting bodies, respectively. The integral equations solved using these approaches can eliminate the interior resonance of dielectric bodies and produce accurate results. The method of moments (MoM) is applied to discretize the integral equations and the resultant matrix system is solved by an iterative solver. The AIM is used then to reduce the memory requirement for storage and to speed up the matrix-vector multiplication in the iterative solver. Numerical results are finally presented to demonstrate the accuracy and efficiency of the technique.

[†] Also with the High Performance Computation for Engineered Systems (HPCES) Programme, Singapore-MIT Alliance (SMA), Kent Ridge, Singapore 119260

1. INTRODUCTION

Integral equation methods have been widely used to solve electromagnetic scattering problems. By using this approach, one has formulated various scattering problems using appropriate integral equations and discretized them using the method of moments (MoM). The MoM procedure converts the integral equation to a system of linear equations which can be solved using either a direct or an iterative solver. The direct solvers, for example, the Gaussian Elimination and LU decomposition methods, require $O(N^3)$ operations while iterative solvers, such as the Gauss-Seidel and Conjugate Gradient techniques, need $O(N^2)$ operations for the matrix-vector multiplication in each iteration. The memory requirement for these two solvers is usually $O(N^2)$. Such computational complexity and memory requirement are too expensive to solve a large-scale scattering problem.

The bottleneck of the iterative solvers is the matrix-vector multiplication during its iteration. Several algorithms have been proposed to speed up the matrix-vector multiplication such as fast multipole method (FMM) [1, 2] and its extensions, multilevel fast multipole algorithm (MLFMA) [3–5] in $O(N^{1.5})$ and $O(N \log N)$, respectively. However, the large constant factor in the asymptotic bound of FMM requires a large value of N in order to gain advantage over the direct MoM. Grid-based solvers such as conjugate-gradient fast Fourier Transform (CG-FFT) method [6] and the pre-corrected fast Fourier Transform (P-FFT) algorithm [7, 8] have been proposed to solve scattering problems of conducting objects. The CG-FFT uses uniform rectangular grids to model arbitrarily shaped geometry, thus it will produce slightly inaccurate results in the final solution due to the staircase approximation. Another powerful grid-based solver is the adaptive integral method (AIM) which was originally proposed by Bleszynski *et al.* to solve electromagnetic scattering problems [9, 10]. It has also been extended to the analysis of radiation problems and large-scale microstrip structures [11, 12]. The computational complexities for the AIM are $O(N^{1.5} \log N)$ and $O(N \log N)$ for surface and volumetric scatterers, respectively.

The analyses of electromagnetic scattering by penetrable dielectric objects have been reported in Ref. [13–15]. However, the proposed methods are limited to characterize small-scaled scattering problems due to the aforementioned reasons. This limitation can be overcome by using a fast algorithm such as AIM although other approaches can also be employed. In this paper, AIM is applied to solve electromagnetic scattering problems of mixed conducting/dielectric bodies which cannot handle easily by the conventional MoM. The

surface integral equation used to define electromagnetic fields in the presence of multiple homogeneous dielectric objects and conducting objects will be formulated using the Poggio-Miller-Chang-Harrington-Wu-Tsai (PMCHWT) formulation [16–18] and electric field integral equation (EFIE) approach, respectively. The resultant integral equations are discretized by using the MoM and by applying the AIM to speed up the matrix-vector multiplication in the iterative solver. Numerical examples are presented to demonstrate the capability of AIM algorithm for analyzing electromagnetic scattering problems of mixed conducting and dielectric objects.

2. FORMULATION

The integral equations for scattering problems of penetrable dielectric scatterers and conducting scatterers are well established and the detailed derivations can be obtained from literature. In this section, a brief introduction to the derivations and a summary of formulations will be given for reader's complete understanding and convenience.

2.1. Mixed Dielectric Objects

First of all, we consider an arbitrarily shaped 3-D scatterer coated by another dielectric material. The scatterer and coating material have different material properties. The object is immersed in a homogeneous medium with permittivity ϵ_1 and permeability μ_1. The interface between media i and j is denoted as S_{ji}, and $S_{ji} = S_{ij}$. The unit vector normal to S_{ji} and pointing toward the medium i is denoted as $\hat{n}_{ji}$. Fig. 1(a) illustrates the notation for an object coated by dielectric material while Fig. 1(b) depicts two discrete objects of different materials.

Using the surface equivalence principle at the interfaces S_{21} and S_{32}, we obtain the electric field integral equations (EFIE) as

$$\hat{n}_{21} \times \bar{E}^i = -\bar{K}_2$$
$$-\hat{n}_{21} \times \left\{ \frac{\nabla\nabla \cdot \bar{A}_{21} + k_1^2 \bar{A}_{21}}{j\omega\epsilon_1} - \nabla \times \bar{F}_{21} \right\} \text{ on } S_{21} \qquad (1a)$$

$$\hat{n}_{21} \times \left\{ \frac{\nabla\nabla \cdot \bar{A}_{32} + k_2^2 \bar{A}_{32}}{-j\omega\epsilon_2} + \nabla \times \bar{F}_{32} \right\} = \bar{K}_2$$
$$-\hat{n}_{21} \times \left\{ \frac{\nabla\nabla \cdot \bar{A}_{22} + k_2^2 \bar{A}_{22}}{j\omega\epsilon_2} - \nabla \times \bar{F}_{22} \right\} \text{ on } S_{21} \qquad (1b)$$
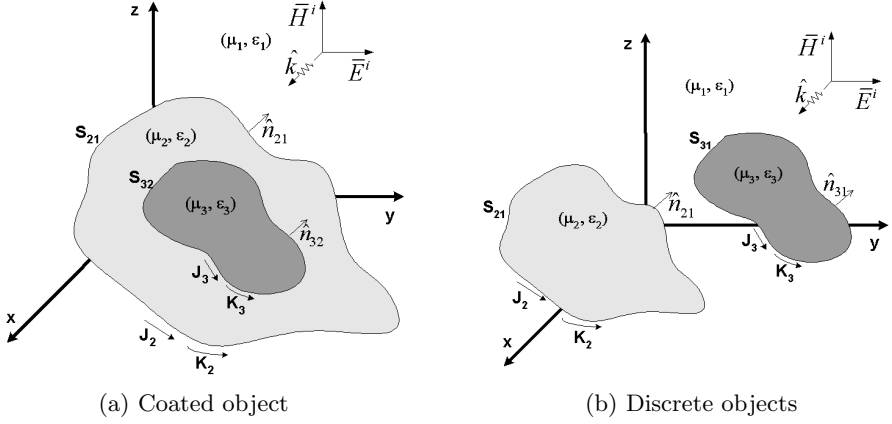
(a) Coated object   (b) Discrete objects

Figure 1. Geometry of a two dielectric scatterers in an isotropic homogeneous medium.

$$\hat{n}_{32} \times \left\{ \frac{\nabla\nabla \cdot \bar{A}_{22} + k_2^2 \bar{A}_{22}}{-j\omega\epsilon_2} + \nabla \times \bar{F}_{22} \right\} = -\bar{K}_3$$

$$-\hat{n}_{32} \times \left\{ \frac{\nabla\nabla \cdot \bar{A}_{32} + k_2^2 \bar{A}_{32}}{j\omega\epsilon_2} - \nabla \times \bar{F}_{32} \right\} \text{ on } S_{32} \qquad (1c)$$

$$0 = \bar{K}_3 - \hat{n}_{32} \times \left\{ \frac{\nabla\nabla \cdot \bar{A}_{33} + k_3^2 \bar{A}_{33}}{j\omega\epsilon_3} - \nabla \times \bar{F}_{33} \right\} \text{ on } S_{32}; \quad (1d)$$

and the magnetic field integral equations (MFIE) as

$$\hat{n}_{21} \times \bar{H}^i = \bar{J}_2$$

$$-\hat{n}_{21} \times \left\{ \nabla \times \bar{A}_{21} + \frac{\nabla\nabla \cdot \bar{F}_{21} + k_1^2 \bar{F}_{21}}{j\omega\mu_1} \right\} \text{ on } S_{21} \qquad (2a)$$

$$\hat{n}_{21} \times \left\{ -\nabla \times \bar{A}_{32} - \frac{\nabla\nabla \cdot \bar{F}_{32} + k_2^2 \bar{F}_{32}}{j\omega\mu_2} \right\} = -\bar{J}_2$$

$$-\hat{n}_{21} \times \left\{ \nabla \times \bar{A}_{22} + \frac{\nabla\nabla \cdot \bar{F}_{22} + k_2^2 \bar{F}_{22}}{j\omega\mu_2} \right\} \text{ on } S_{21} \qquad (2b)$$

$$\hat{n}_{32} \times \left\{ -\nabla \times \bar{A}_{22} - \frac{\nabla\nabla \cdot \bar{F}_{22} + k_2^2 \bar{F}_{22}}{j\omega\mu_2} \right\} = \bar{J}_3$$

$$-\hat{n}_{32} \times \left\{ \nabla \times \bar{A}_{32} + \frac{\nabla\nabla \cdot \bar{F}_{32} + k_2^2 \bar{F}_{32}}{j\omega\mu_2} \right\} \text{ on } S_{32} \qquad (2c)$$

$$0 = -\bar{J}_3 - \hat{n}_{32} \times \left\{ \nabla \times \bar{A}_{33} + \frac{\nabla\nabla \cdot \bar{F}_{33} + k_3^2 \bar{F}_{33}}{j\omega\mu_3} \right\} \quad \text{on } S_{32}; \quad (2d)$$

where the vector potentials $\bar{A}_{ji}$ and $\bar{F}_{ji}$ are given by

$$\bar{A}_{ji} = \iint \bar{J}_j g_i\left(\mathbf{r}, \mathbf{r}'\right) dS \tag{3}$$

$$\bar{F}_{ji} = \iint \bar{K}_j g_i\left(\mathbf{r}, \mathbf{r}'\right) dS \tag{4}$$

$$g_i\left(\mathbf{r}, \mathbf{r}'\right) = \frac{e^{-jk_i|\mathbf{r}-\mathbf{r}'|}}{4\pi|\mathbf{r} - \mathbf{r}'|} \tag{5}$$

with j is the subscript of the equivalent source current and i denotes the medium into which the equivalent source current radiates, and the wavenumber is obtained as $k_i = \omega\sqrt{\mu_i\epsilon_i}$. The $\bar{J}_j$ and $\bar{K}_j$ are the equivalent surface electric and magnetic currents defined by

$$\bar{J}_j = \hat{n}_{ji} \times \bar{H} \text{ on } S_{ji} \tag{6}$$

$$\bar{K}_j = \bar{E} \times \hat{n}_{ji} \text{ on } S_{ji}. \tag{7}$$

Using the PMCHWT approach, we combine the Eqs. (1a)–(1d) and (2a)–(2d) and obtain

$$\hat{n}_{21} \times \bar{E}^i = -\hat{n}_{21} \times \left\{ \frac{\nabla\nabla \cdot \bar{A}_{21} + k_1^2 \bar{A}_{21}}{j\omega\epsilon_1} + \frac{\nabla\nabla \cdot \bar{A}_{22} + k_2^2 \bar{A}_{22}}{j\omega\epsilon_2} \right.$$
$$\left. -\nabla \times \bar{F}_{21} - \nabla \times \bar{F}_{22} - \frac{\nabla\nabla \cdot \bar{A}_{32} + k_2^2 \bar{A}_{32}}{j\omega\epsilon_2} + \nabla \times \bar{F}_{32} \right\} \quad (8a)$$

$$\hat{n}_{21} \times \bar{H}^i = -\hat{n}_{21} \times \left\{ \nabla \times \bar{A}_{21} + \nabla \times \bar{A}_{22} + \frac{\nabla\nabla \cdot \bar{F}_{21} + k_1^2 \bar{F}_{21}}{j\omega\mu_1} \right.$$
$$\left. +\frac{\nabla\nabla \cdot \bar{F}_{22} + k_2^2 \bar{F}_{22}}{j\omega\mu_2} - \nabla \times \bar{A}_{32} - \frac{\nabla\nabla \cdot \bar{F}_{32} + k_2^2 \bar{F}_{32}}{j\omega\mu_2} \right\} \quad (8b)$$

$$0 = -\hat{n}_{32} \times \left\{ -\frac{\nabla\nabla \cdot \bar{A}_{22} + k_2^2 \bar{A}_{22}}{j\omega\epsilon_2} + \nabla \times \bar{F}_{22} + \frac{\nabla\nabla \cdot \bar{A}_{32} + k_2^2 \bar{A}_{32}}{j\omega\epsilon_2} \right.$$
$$\left. + \frac{\nabla\nabla \cdot \bar{A}_{33} + k_3^2 \bar{A}_{33}}{j\omega\epsilon_3} - \nabla \times \bar{F}_{32} - \nabla \times \bar{F}_{33} \right\} \quad (8c)$$

$$0 = -\hat{n}_{32} \times \left\{ -\nabla \times \bar{A}_{22} - \frac{\nabla\nabla \cdot \bar{F}_{22} + k_2^2 \bar{F}_{22}}{j\omega\mu_2} + \nabla \times \bar{A}_{32} + \nabla \times \bar{A}_{33} \right.$$
$$\left. + \frac{\nabla\nabla \cdot \bar{F}_{32} + k_2^2 \bar{F}_{32}}{j\omega\mu_2} + \frac{\nabla\nabla \cdot \bar{F}_{33} + k_3^2 \bar{F}_{33}}{j\omega\mu_3} \right\}. \quad (8d)$$

Next we consider the discrete scatterers as shown in Fig. 1(b). Applying the same procedure, we can obtain

$$
\hat{n}_{21} \times \bar{E}^i = -\hat{n}_{21} \times \left\{ \frac{\nabla\nabla \cdot \bar{A}_{21} + k_1^2 \bar{A}_{21}}{j\omega\epsilon_1} + \frac{\nabla\nabla \cdot \bar{A}_{22} + k_2^2 \bar{A}_{22}}{j\omega\epsilon_2} \right.
$$
$$
\left. -\nabla \times \bar{F}_{21} - \nabla \times \bar{F}_{22} + \frac{\nabla\nabla \cdot \bar{A}_{31} + k_1^2 \bar{A}_{31}}{j\omega\epsilon_1} - \nabla \times \bar{F}_{31} \right\} \qquad (9a)
$$

$$
\hat{n}_{21} \times \bar{H}^i = -\hat{n}_{21} \times \left\{ \nabla \times \bar{A}_{21} + \nabla \times \bar{A}_{22} + \frac{\nabla\nabla \cdot \bar{F}_{21} + k_1^2 \bar{F}_{21}}{j\omega\mu_1} \right.
$$
$$
\left. + \frac{\nabla\nabla \cdot \bar{F}_{22} + k_2^2 \bar{F}_{22}}{j\omega\mu_2} + \nabla \times \bar{A}_{31} + \frac{\nabla\nabla \cdot \bar{F}_{31} + k_1^2 \bar{F}_{31}}{j\omega\mu_1} \right\} \qquad (9b)
$$

$$
\hat{n}_{31} \times \bar{E}^i = -\hat{n}_{31} \times \left\{ \frac{\nabla\nabla \cdot \bar{A}_{21} + k_1^2 \bar{A}_{21}}{j\omega\epsilon_1} - \nabla \times \bar{F}_{21} \right.
$$
$$
\left. + \frac{\nabla\nabla \cdot \bar{A}_{31} + k_1^2 \bar{A}_{31}}{j\omega\epsilon_1} + \frac{\nabla\nabla \cdot \bar{A}_{33} + k_3^2 \bar{A}_{33}}{j\omega\epsilon_3} - \nabla\times\bar{F}_{31} - \nabla\times\bar{F}_{33} \right\} \qquad (9c)
$$

$$
\hat{n}_{31} \times \bar{H}^i = -\hat{n}_{31} \times \left\{ \nabla \times \bar{A}_{21} + \frac{\nabla\nabla \cdot \bar{F}_{21} + k_1^2 \bar{F}_{21}}{j\omega\mu_1} + \nabla \times \bar{A}_{31} \right.
$$
$$
\left. + \nabla \times \bar{A}_{33} + \frac{\nabla\nabla \cdot \bar{F}_{31} + k_1^2 \bar{F}_{31}}{j\omega\mu_1} + \frac{\nabla\nabla \cdot \bar{F}_{33} + k_3^2 \bar{F}_{33}}{j\omega\mu_3} \right\}. \qquad (9d)
$$

2.2. Mixed Conducting-Dielectric Body

Now, we replace the core of the coated object with a perfectly conducting scatterer as shown in Fig. 2(a) and the material properties of the coating layer are characterized by ϵ_2 and μ_2. By applying the surface equivalence principle on the surface S_{21} and S_{02}, we obtain the EFIE as

$$
\hat{n}_{21} \times \bar{E}^i = -\bar{K}_2
$$
$$
-\hat{n}_{21} \times \left\{ \frac{\nabla\nabla \cdot \bar{A}_{21} + k_1^2 \bar{A}_{21}}{j\omega\epsilon_1} - \nabla \times \bar{F}_{21} \right\} \text{ on } S_{21} \qquad (10a)
$$

$$
\hat{n}_{21} \times \left\{ \frac{\nabla\nabla \cdot \bar{A}_{02} + k_2^2 \bar{A}_{02}}{-j\omega\epsilon_2} \right\} = \bar{K}_2
$$
$$
-\hat{n}_{21} \times \left\{ \frac{\nabla\nabla \cdot \bar{A}_{22} + k_2^2 \bar{A}_{22}}{j\omega\epsilon_2} - \nabla \times \bar{F}_{22} \right\} \text{ on } S_{21} \qquad (10b)
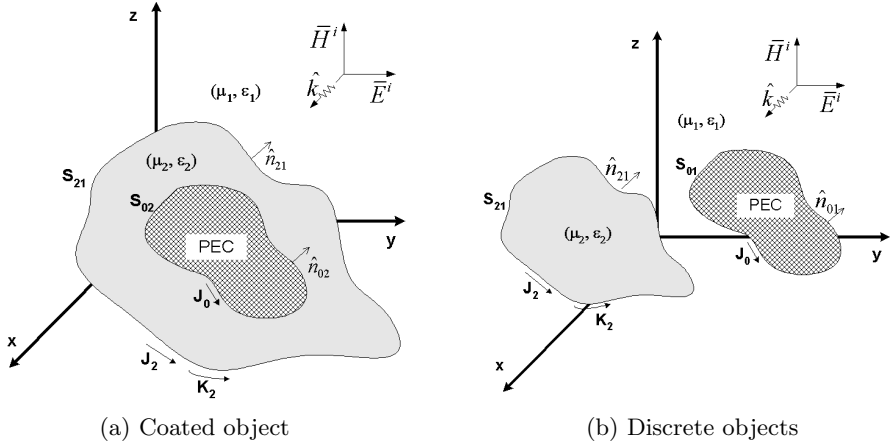$$

(a) Coated object

(b) Discrete objects

Figure 2. Geometry of a dielectric and perfectly conducting scatterers in an isotropic homogeneous medium.

$$\hat{n}_{02} \times \left\{ \frac{\nabla\nabla \cdot \bar{A}_{22} + k_2^2 \bar{A}_{22}}{-j\omega\epsilon_2} + \nabla \times \bar{F}_{22} \right\} =$$

$$-\hat{n}_{02} \times \left\{ \frac{\nabla\nabla \cdot \bar{A}_{02} + k_2^2 \bar{A}_{02}}{j\omega\epsilon_2} \right\} \quad \text{on } S_{02} \tag{10c}$$

and the MFIE as

$$\hat{n}_{21} \times \bar{H}^i = \bar{J}_2$$
$$-\hat{n}_{21} \times \left\{ \nabla \times \bar{A}_{21} + \frac{\nabla\nabla \cdot \bar{F}_{21} + k_1^2 \bar{F}_{21}}{j\omega\mu_1} \right\} \quad \text{on } S_{21} \tag{11a}$$

$$\hat{n}_{21} \times \left\{ -\nabla \times \bar{A}_{02} \right\} = -\bar{J}_2$$
$$-\hat{n}_{21} \times \left\{ \nabla \times \bar{A}_{22} + \frac{\nabla\nabla \cdot \bar{F}_{22} + k_2^2 \bar{F}_{22}}{j\omega\mu_2} \right\} \quad \text{on } S_{21} \tag{11b}$$

$$\hat{n}_{02} \times \left\{ -\nabla \times \bar{A}_{22} - \frac{\nabla\nabla \cdot \bar{F}_{22} + k_2^2 \bar{F}_{22}}{j\omega\mu_2} \right\} = \bar{J}_0$$
$$-\hat{n}_{02} \times \left\{ \nabla \times \bar{A}_{02} \right\} \quad \text{on } S_{02}; \tag{11c}$$

Using PMCHWT approach, we combine Eqs. (10a)–(10b) and (11a)–(11b) to obtain

$$\hat{n}_{21} \times \bar{E}^i = -\hat{n}_{21} \times \left\{ \frac{\nabla\nabla \cdot \bar{A}_{21} + k_1^2 \bar{A}_{21}}{j\omega\epsilon_1} + \frac{\nabla\nabla \cdot \bar{A}_{22} + k_2^2 \bar{A}_{22}}{j\omega\epsilon_2} \right.$$

$$-\nabla \times \bar{F}_{21} - \nabla \times \bar{F}_{22} - \frac{\nabla\nabla \cdot \bar{A}_{02} + k_2^2 \bar{A}_{02}}{j\omega\epsilon_2}\Bigg\} \tag{12a}$$

$$\hat{n}_{21} \times \bar{H}^i = -\hat{n}_{21} \times \Bigg\{ \nabla \times \bar{A}_{21} + \nabla \times \bar{A}_{22}$$

$$+ \frac{\nabla\nabla \cdot \bar{F}_{21} + k_1^2 \bar{F}_{21}}{j\omega\mu_1} + \frac{\nabla\nabla \cdot \bar{F}_{22} + k_2^2 \bar{F}_{22}}{j\omega\mu_2} - \nabla \times \bar{A}_{02} \Bigg\} \tag{12b}$$

Next we consider the conducting scatterer placed beside a discrete dielectric scatterer as shown in Fig. 2(b). Following the same procedure, we can obtain the following equations:

$$\hat{n}_{21} \times \bar{E}^i = -\hat{n}_{21} \times \Bigg\{ \frac{\nabla\nabla \cdot \bar{A}_{21} + k_1^2 \bar{A}_{21}}{j\omega\epsilon_1} + \frac{\nabla\nabla \cdot \bar{A}_{22} + k_2^2 \bar{A}_{22}}{j\omega\epsilon_2}$$

$$-\nabla \times \bar{F}_{21} - \nabla \times \bar{F}_{22} + \frac{\nabla\nabla \cdot \bar{A}_{01} + k_1^2 \bar{A}_{01}}{j\omega\epsilon_1} \Bigg\} \tag{13a}$$

$$\hat{n}_{21} \times \bar{H}^i = -\hat{n}_{21} \times \Big\{ \nabla \times \bar{A}_{21} + \nabla \times \bar{A}_{22}$$

$$+ \frac{\nabla\nabla \cdot \bar{F}_{21} + k_1^2 \bar{F}_{21}}{j\omega\mu_1} + \frac{\nabla\nabla \cdot \bar{F}_{22} + k_2^2 \bar{F}_{22}}{j\omega\mu_2} + \nabla \times \bar{A}_{01} \Bigg\} \tag{13b}$$

$$\hat{n}_{01} \times \bar{E}^i = -\hat{n}_{01} \times \Bigg\{ \frac{\nabla\nabla \cdot \bar{A}_{21} + k_1^2 \bar{A}_{21}}{j\omega\epsilon_1}$$

$$-\nabla \times \bar{F}_{21} + \frac{\nabla\nabla \cdot \bar{A}_{01} + k_1^2 \bar{A}_{01}}{j\omega\epsilon_1} \Bigg\} \tag{13c}$$

2.3. Method of Moments

The integral equations given in the previous subsections are discretized using method of moments. The arbitrarily shaped 3D objects in this paper are modeled using triangular patches. Hence it is convenient to use the planar triangular basis functions or Rao-Wilton-Glisson (RWG) basis functions f_n [19] to expand the equivalent surface electric and magnetic currents $\bar{J}_i$ and $\bar{K}_i$ ($i = 2$ or 3) as follows:

$$\bar{J}_i = \sum I_{n_{i-1}} f_{n_{i-1}} \tag{14a}$$

$$\bar{K}_i = \sum M_{n_{i-1}} f_{n_{i-1}}. \tag{14b}$$

Substituting Eqs. (14a)–(14b) into (8a)–(8d) and (9a)–(9d), and applying the Galerkin's testing procedure, we convert the integral

equations to a linear equation system written as

$$
\begin{bmatrix}
[Z_{mn}^{11}] & [C_{mn}^{11}] & \theta\,[Z_{mn}^{12}] & \theta\,[C_{mn}^{12}] \\
[D_{mn}^{11}] & [Y_{mn}^{11}] & \theta\,[D_{mn}^{12}] & \theta\,[Y_{mn}^{12}] \\
\theta\,[Z_{mn}^{21}] & \theta\,[C_{mn}^{21}] & [Z_{mn}^{22}] & [C_{mn}^{22}] \\
\theta\,[D_{mn}^{21}] & \theta\,[Y_{mn}^{21}] & [D_{mn}^{22}] & [Y_{mn}^{22}]
\end{bmatrix}
\begin{bmatrix}
[I_1] \\
[M_1] \\
[I_2] \\
[M_2]
\end{bmatrix}
=
\begin{bmatrix}
[E_m^1] \\
[H_m^1] \\
\delta\,[E_m^2] \\
\delta\,[H_m^2]
\end{bmatrix}
$$

(15)

where the $([I_1],[M_1])$ and $([I_2],[M_2])$ are the coefficients of the equivalent electric and magnetic currents on S_{2i} and S_{3i}, respectively. The elements of the sub-matrices, for $u \neq v$, are defined as

$$
Z_{mn}^{uv} = -\int_{T_{m_u}} f_{m_u}(\mathbf{r}) \cdot \left(j\omega\mu_a P_{n_v}^a + \frac{j}{\omega\epsilon_a} Q_{n_v}^a \right) dS_{m_u}
\qquad (16a)
$$

$$
Y_{mn}^{uv} = -\int_{T_{m_u}} f_{m_u}(\mathbf{r}) \cdot \left(j\omega\epsilon_a P_{n_v}^a + \frac{j}{\omega\mu_a} Q_{n_v}^a \right) dS_{m_u}
\qquad (16b)
$$

$$
C_{mn}^{uv} = -\int_{T_{m_u}} f_{m_u}(\mathbf{r}) \cdot \left(\nabla \times P_{n_v}^a \right) dS_{m_u}
\qquad (16c)
$$

$$
D_{mn}^{uv} = -C_{mn}^{uv}
\qquad (16d)
$$

and for $u = v$, as:

$$
Z_{mn}^{uu} = \int_{T_{m_u}} f_{m_u}(\mathbf{r}) \cdot \left(j\omega\mu_b P_{n_u}^b + \frac{j}{\omega\epsilon_b} Q_{n_u}^b \right.
$$
$$
\left. + j\omega\mu_{u+1} P_{n_u}^{u+1} + \frac{j}{\omega\epsilon_{u+1}} Q_{n_u}^{u+1} \right) dS_{m_u}
\qquad (17a)
$$

$$
Y_{mn}^{uu} = \int_{T_{m_u}} f_{m_u}(\mathbf{r}) \cdot \left(j\omega\epsilon_b P_{n_u}^b + \frac{j}{\omega\mu_b} Q_{n_u}^b \right.
$$
$$
\left. + j\omega\epsilon_{u+1} P_{n_u}^{u+1} + \frac{j}{\omega\mu_{u+1}} Q_{n_u}^{u+1} \right) dS_{m_u}
\qquad (17b)
$$

$$
C_{mn}^{uu} = \int_{T_{m_u}} f_{m_u}(\mathbf{r}) \cdot \left(\nabla \times P_{n_u}^b + \nabla \times P_{n_u}^{u+1} \right) dS_{m_u}
\qquad (17c)
$$

$$
D_{mn}^{uu} = -C_{mn}^{uu}
\qquad (17d)
$$

where

$$
P_{n_v}^u = \int_{T_{n_v}} f_{n_v}(\mathbf{r}') g_u(\mathbf{r}, \mathbf{r}') dS_{n_v}
\qquad (18)
$$

$$Q_{n_v}^u = \nabla \int\limits_{T_{n_v}} \nabla_s' \cdot f_{n_v}(\mathbf{r}')g_u\,(\mathbf{r},\mathbf{r}')\,dS_{n_v}. \tag{19}$$

and the symbols, μ_u and ϵ_u, denote the permeability and permittivity in medium u, respectively. The elements of the excitation electric and magnetic fields are expressed as

$$E_m^u = \int\limits_{T_{m_u}} f_{m_u} \cdot \bar{E}^i dS_{m_u} \tag{20a}$$

$$H_m^u = \int\limits_{T_{m_u}} f_{m_u} \cdot \bar{H}^i dS_{m_u} \tag{20b}$$

For the problems discussed in subsection 1, we let $(\delta = 0,\ \theta = 1,\ a = 2,\ b = u)$ and $(\delta = 1,\ \theta = -1,\ a = 1,\ b = 1)$ for cases shown in Fig. 1(a) and 1(b), respectively. As for the problems discussed in subsection 2, the conversion of integral equations to a matrix equation is straightforward using the same procedure. The elements of sub-matrices can be deduced easily from (12a)–(12b) and (10c), and (13a)–(13c).

2.4. Adaptive Integral Method

The AIM was proposed to reduce the memory requirement and to accelerate the matrix-vector multiplication process in an iterative solver. The basic idea of the AIM is to approximate the far-zone interaction using the fast Fourier Transform (FFT), and to calculate the near-field interaction directly in order to reduce the computational time. The matrix-vector multiplication can be split into two parts, *i.e.*,

$$[Z][I]=[Z^{near}][I]+[Z^{far}][I]$$

where $[Z^{near}]$ denotes a sparse matrix that contains only the nearby elements within a threshold distance and $[Z^{far}]$ represents the far-zone interaction of the elements.

To employ AIM, the object is enclosed in a rectangular grid and is then recursively subdivided into small rectangular grids. We need to transform the RWG basis functions to the surrounding Cartesian grids in order to use the FFT to approximate the far-zone interaction. We note that all the matrix elements can be expressed in the following unified form

$$Z_{mn} = \int\limits_{T_m} \int\limits_{T_n} \gamma_m\,(\mathbf{r})g(\mathbf{r},\mathbf{r}')\gamma_n(\mathbf{r}')dr'dr \tag{21}$$

where $\gamma_n(\mathbf{r}) = \{f_n(\mathbf{r}), \nabla \cdot f_n(\mathbf{r}), \nabla \times f_n(\mathbf{r})\}$. The $\gamma_n(\mathbf{r})$ can be certainly approximated as a linear combination of Dirac delta functions,

$$\gamma_n(\mathbf{r}) \approx \hat{\gamma}_n(\mathbf{r}) = \sum_{v=1}^{(M+1)^3} \Lambda_{nv} \delta(\mathbf{r} - \mathbf{r}') \tag{22}$$

where M is the expansion order, and Λ_{nv} denotes the expansion coefficients of $\gamma_n(\mathbf{r})$, which can be determined by using multipole expansion [10] or far-field approximation [11]. The multipole expansion method is based on the criteria that the coefficients Λ_{nv} produce the same multipole moments of the original basis function

$$\sum_{v=1}^{(M+1)^3} (x_{nv} - x_0)^{m1} (y_{nv} - y_0)^{m2} (z_{nv} - z_0)^{m3} \Lambda_{nv}$$
$$= \int_{T_n} \gamma_n(\mathbf{r}) (x - x_0)^{m1} (y - y_0)^{m2} (z - z_0)^{m3} dS_n \tag{23}$$
$$\text{for } 0 \leq \{m1, m2, m3\} \leq M$$

where the reference point $r_0 = (x_0, y_0, z_0)$ is chosen as the centre of the basis function. The far-field approximation method matches the far-field produced by $\gamma_n(\mathbf{r})$ and $\hat{\gamma}_n(\mathbf{r})$ on a unit sphere, and thus the expansion coefficients are obtained. Once the transformation functions are determined, the matrix elements can be approximated as

$$\hat{Z}_{mn} = \sum_{u=1}^{(M+1)^3} \sum_{v=1}^{(M+1)^3} \Lambda_{mu} g(\mathbf{r_u}, \mathbf{r_v}') \Lambda_{nv}. \tag{24}$$

By using the approximation, now we are able to compute two components in the matrix-vector multiplication with

$$Z^{far} = \Lambda g \Lambda^T \tag{25a}$$
$$Z^{near} = Z_{nz}^{MoM} - Z^{far} \tag{25b}$$

where Z_{nz}^{MoM} is the matrix containing only the direct interaction of neighbor elements and Λ represents the basis transformation matrix of the elements. The $[g]$ is Toeplitz, and this enables the use of FFT to compute the 3D convolution in (25a) efficiently. Hence we can represent the matrix-vector multiplication as

$$ZI = Z^{near} I + Z^{far} I$$
$$= Z^{near} I + \Lambda \mathcal{F}^{-1} \left\{ \mathcal{F}\{g\} \cdot \mathcal{F}\left\{\Lambda^T I\right\} \right\} \tag{26}$$

where $\mathcal{F}\{\bullet\}$ and $\mathcal{F}^{-1}\{\bullet\}$ are FFT and inverse FFT, respectively.

3. NUMERICAL RESULT

In this section, several examples will be presented to show the accuracy of the proposed method and correctness of the developed algorithms. All the computations are carried out on a Pentium IV personal computer and the generalized minimum residual (GMRES) solver is used. The relative error norm of 10^{-3} is used in the solver to terminate the iterations. The first example is computed using the far-field approximation while other examples are computed using the multipole expansion technique.

The first three examples are considered for validating the accuracy of the code developed while the remaining examples are considered to produce some new results which cannot be found elsewhere in literature. The first example we consider is a coated dielectric sphere having a radius of $1\,\mathrm{m}$. The core of the sphere has a radius of $0.9\,\mathrm{m}$ and a relative permittivity of $\epsilon_{r1} = 1.4 - j0.3$, and the thickness of coating layer is $0.1\,\mathrm{m}$ with a relative permittivity of $\epsilon_{r2} = 1.6 - j0.8$. The bistatic RCSs for the VV- and HH-polarizations at $750\,\mathrm{MHz}$ are computed and the results are shown in Fig. 3. The results are compared with Mie series solutions and good agreements have been observed in the comparisons.
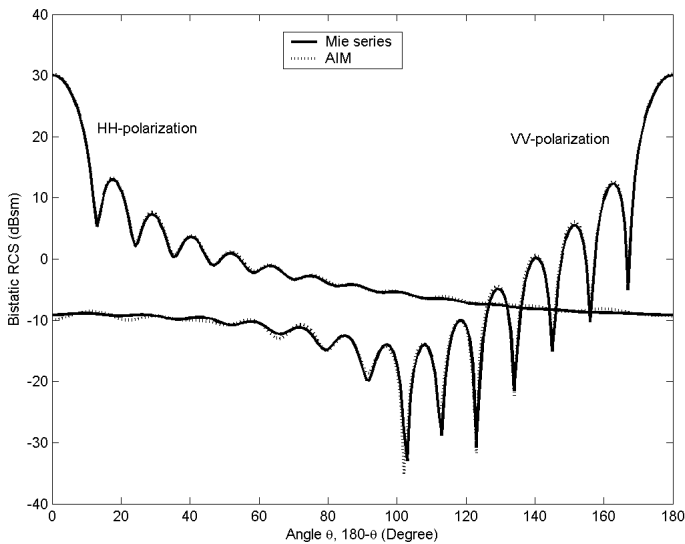

Figure 3. Bistatic RCS of a coated dielectric sphere ($a_1 = 0.9\,\mathrm{m}$, $\epsilon_{r1} = 1.4 - j0.3$; $a_2 = 1\,\mathrm{m}$, $\epsilon_{r2} = 1.6 - j0.8$) at $750\,\mathrm{MHz}$.
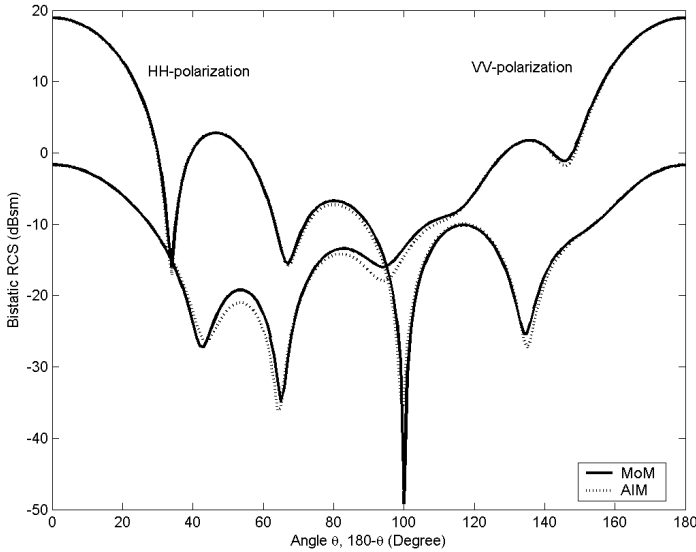
Figure 4. Bistatic RCS of a $1\,\text{m} \times 1\,\text{m} \times 1\,\text{m}$ dielectric cube ($\epsilon_r = 1.6 - j0.4$) at $450\,\text{MHz}$.

The second example is a $1\,\text{m} \times 1\,\text{m} \times 1\,\text{m}$ dielectric cube with relative permittivity of $\epsilon_r = 1.6 - j0.4$. The bistatic RCSs for VV- and HH-polarizations of this cube at $450\,\text{MHz}$ are computed considering 9100 unknowns and the results are compared with the MoM solutions in Fig. 4. A good agreement is also observed between the results.

The third example we consider is a coated conducting sphere having a radius of $1\,\text{m}$. The conducting core has a radius $0.9\,\text{m}$ and the thickness of the coating layer is $0.1\,\text{m}$ with relative permittivity of $\epsilon_r = 1.6 - j0.8$. The bistatic RCSs for VV- and HH-polarizations are computed considering 45540 unknowns and the results are shown in Fig. 5. The results are compared with Mie series solution and a good agreement is observed.

The fourth example considered is a PEC-dielectric cylinder. The diameter of the cylinder is $7.62\,\text{cm}$ while the length of the PEC and dielectric cylinders are $5.08\,\text{cm}$ each. The monostatic RCSs for VV- and HH-polarizations are computed at $3\,\text{GHz}$ and $10\,\text{GHz}$, and are shown in Fig. 6. The RCSs computed at $3\,\text{GHz}$ agree well with the published results [13].

The fifth example analyzed is the scattering by two dielectric spheres with different radii. The spheres are only radiatively closely
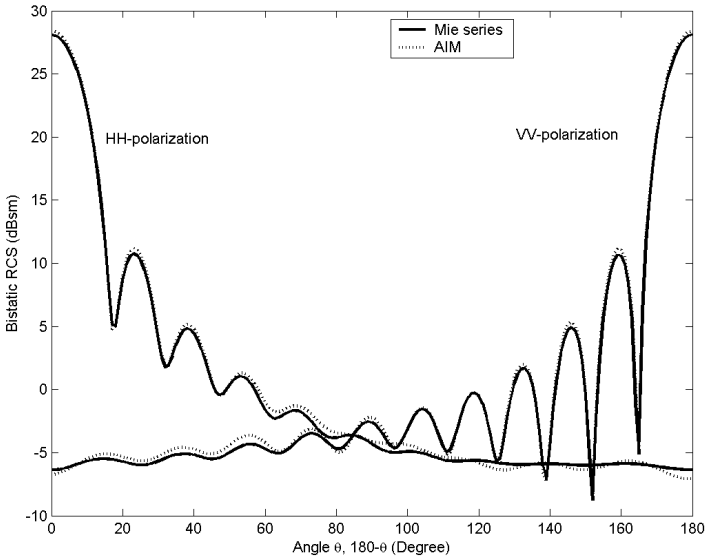
Figure 5. Bistatic RCS of a coated conducting sphere ($a_1 = 0.9\,\mathrm{m}$; $a_2 = 1\,\mathrm{m}$, $\epsilon_r = 1.6 - j0.8$) at $600\,\mathrm{MHz}$.

coupled and the relative permittivities of the spheres respectively placed right and left in Fig. 7 are $1.75 - j0.3$ and $2.25 - j0.5$. The bistatic RCSs for VV- and HH-polarizations are shown in Fig. 7. The RCSs of the spheres with radius of 0.4λ are compared with those in [14] and a good agreement is observed. The sixth example is the scattering by nine agglomerated spheres, of which five spheres have $\epsilon_{r1} = 1.75 - j0.3$ and four spheres have $\epsilon_{r2} = 2.25 - j0.5$. Resulted from 90060 unknowns, the bistatic RCSs for VV- and HH- polarizations are obtained and shown in Fig. 8.

The last example considered is a system consisting of four agglomerated dielectric spheres on the top of a PEC plate. The diameter of each of the four spheres is 2λ and the relative permittivity of each of the spheres is $1.6 - j0.4$. The $8\lambda \times 8\lambda$ PEC plate is placed at $z = 0$ and the centers of the spheres are located 1.3λ above the PEC plate. The scattering of plane waves by the spheres in the presence and absence of the finite PEC plate are computed and shown in Fig. 9. As expected, the RCS is higher for the case in the presence of the PEC plate.
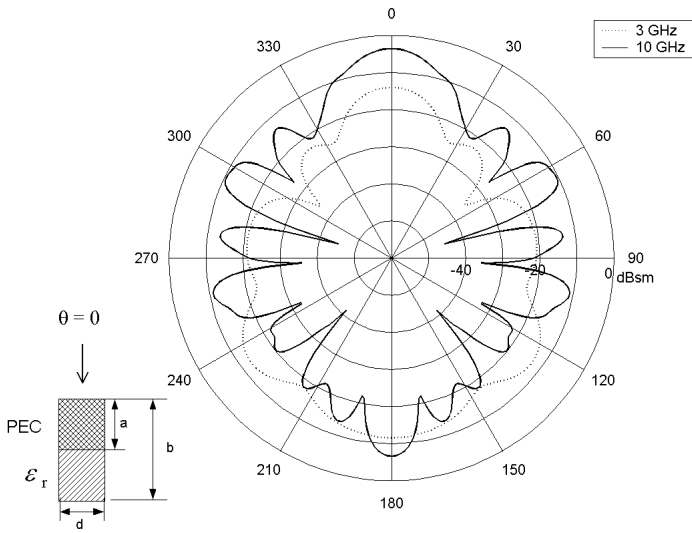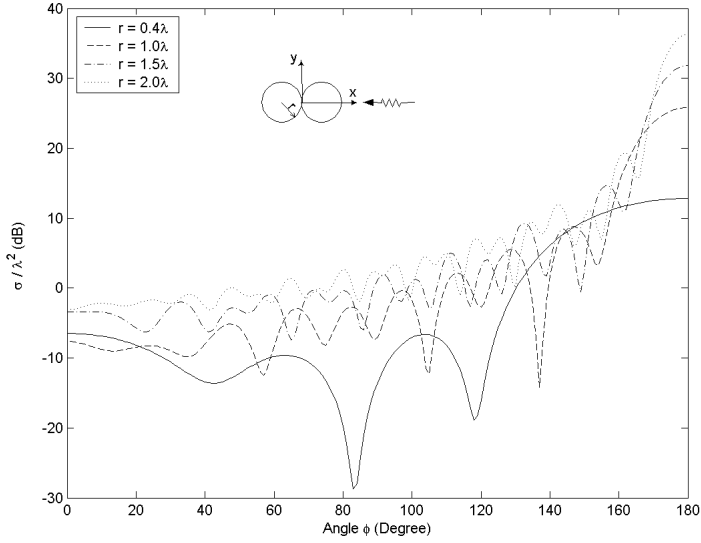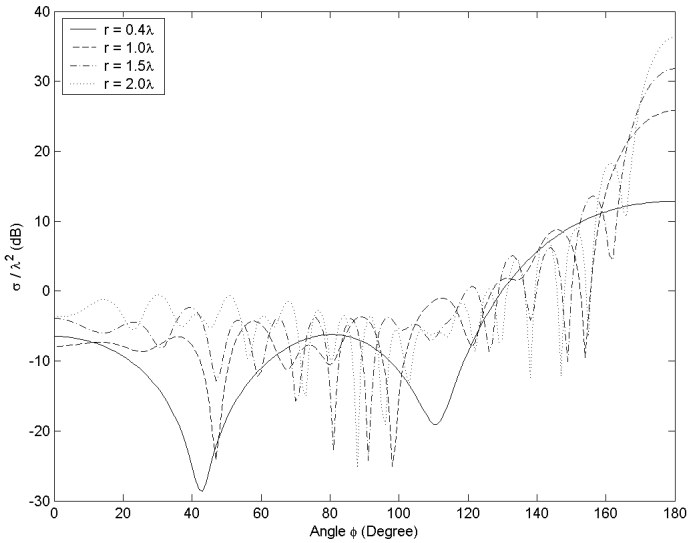
(a) VV-polarization
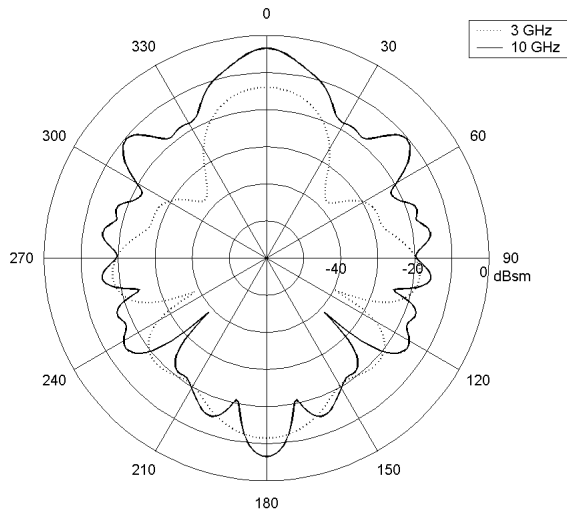
(b) HH-polarization

Figure 6. Monostatic RCS of a PEC-dielectric cylinder ($a = 5.08$ cm, $b = 10.16$ cm, $d = 7.62$ cm, and $\epsilon_r = 2.6$).

(a) VV-polarization

(b) HH-polarization

Figure 7. Bistatic RCS of two dielectric spheres ($\epsilon_{r1} = 1.75 - j0.3$, and $\epsilon_{r2} = 2.25 - j0.5$) with different radii.
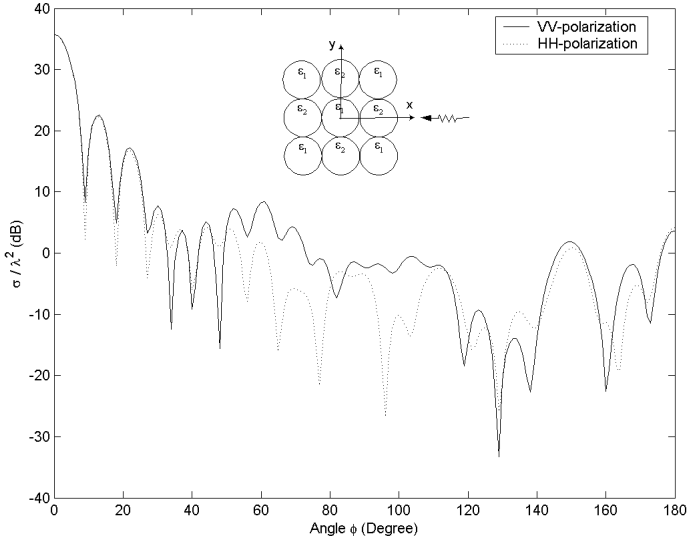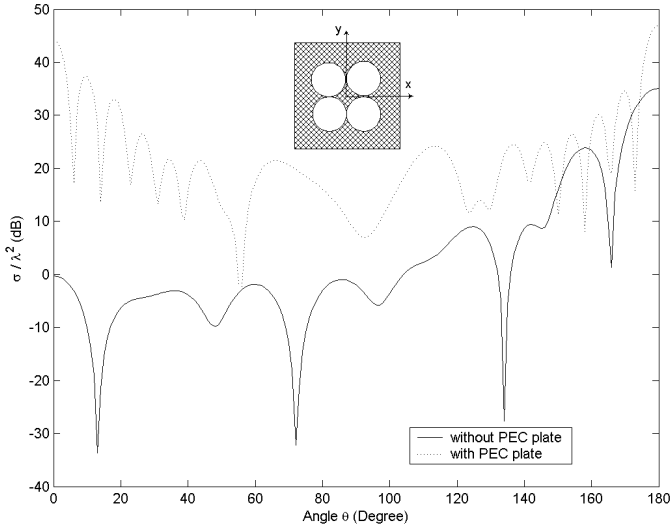
Figure 8. Bistatic RCS of nine dielectric spheres, each of diameter 2λ ($\epsilon_{r1} = 1.75 - j0.3$, and $\epsilon_{r2} = 2.25 - j0.5$).

4. CONCLUSION

In this paper, the AIM has been extended to solve electromagnetic scattering by mixed dielectric/conducting bodies. The problem is formulated using the PMCHWT and EFIE approaches for dielectric and conducting bodies, respectively. After the resultant integral equations are discretized using the MoM, the AIM is employed to reduce the memory requirement and to speed up the matrix-vector multiplication in the iterative solver. Numerical results are presented to demonstrate the accuracy and capability of the proposed method. Simple tests are conducted by firstly comparing the results obtained from the present method with Mie scattering exact results, and by secondly comparing the present results with those results from the standard MoM. Fairly good agreements were found in the comparison.

ACKNOWLEDGMENT
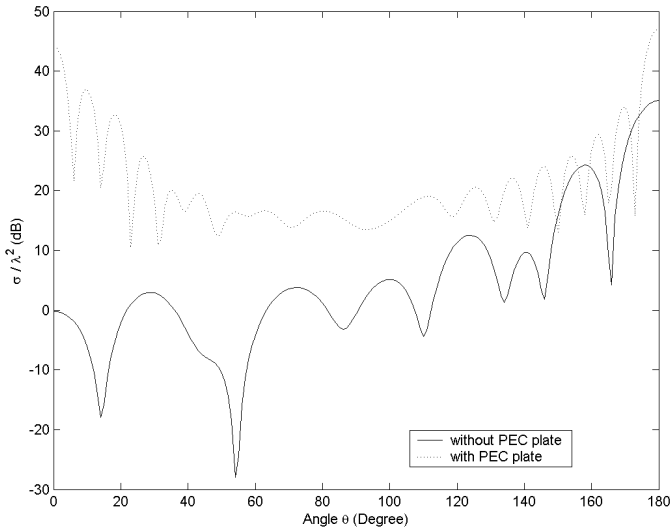
(a) VV-polarization

(b) HH-polarization

Figure 9. Bistatic RCS of four agglomerated dielectric spheres ($r = 1\lambda$, $\epsilon_r = 1.6 - j0.4$) in the presence and absence of a $8\lambda \times 8\lambda$ PEC plate.

REFERENCES

1. Rokhlin, V., "Rapid solution of integral equation of scattering theory in two dimensions," *J. Comput. Phys.*, Vol. 86, 414–439, Feb. 1990.

2. Coifman, R., V. Rokhlin, and S. Wandzura, "The fast multipole method for the wave equation: A pedestrian prescription," *IEEE Antennas Propagat. Mag.*, Vol. 35, 7–12, June 1993.

3. Lu, C. C. and W. C. Chew, "A multilevel algorithm for solving boundary integral equations of wave scattering," *Microwave Opt. Tech. Lett.*, Vol. 7, No. 10, 466–470, July 1994.

4. Song, J. M. and W. C. Chew, "Multilevel fast-multipole algorithm for solving combined field integral equations of electromagnetics scattering," *Microwave Opt. Tech. Lett.*, Vol. 10, No. 1, 14–19, Sept. 1995.

5. Song, J. M., C. C. Lu, and W. C. Chew, "Multilevel fast multipole algorithm for electromagnetic scattering by large complex objects," *IEEE Trans. Antennas Propagat.*, Vol. 45, No. 10, 1488–1493, Oct. 1997.

6. Sarkar, T. K., E. Arvas, and S. M. Rao, "Application of FFT and the conjugate gradient method for the solution of electromagnetic radiation from electrically large and small conducting bodies," *IEEE Trans. Antennas Propagat.*, Vol. 34, No. 5, 635–640, May 1986.

7. Nie, X. C., L. W. Li, N. Yuan, and Y. T. Soon, "Precorrected-FFT algorithm for solving combined field integral equations in electromagnetic scattering," *J. Electromag. Waves Applicat.*, Vol. 16, No. 8, 1171–1187, August 2002.

8. Nie, X. C., L.W. Li, N. Yuan, Y. T. Soon, and Y. B. Gan, "Fast analysis of scattering by arbitrarily shaped three-dimensional objects using the precorrected-FFT method," *Microwave Opt. Tech. Lett.*, Vol. 34, No. 6, 438–442, Sept. 2002.

9. Bleszynski, E., M. Bleszynski, and T. Jaroszewicz, "A fast integral equation solver for electromagnetic scattering problems," *IEEE APS Int. Symp. Dig.*, Vol. 1, 416–419, 1994.

10. Bleszynski, E., M. Bleszynski, and T. Jaroszewicz, "AIM: adaptive integral method for solving large-scale electromagnetic scattering and radiation problems," *Radio Sci.*, Vol. 31, 1225–1251, Sept.–Oct. 1996.

11. Ling, F., C. F. Wang, and J. M. Jin, "Application of adaptive integral method to scattering and radiation analysis of arbitrarily shaped planar structures," *J. Electromag. Waves Applicat.*,

Vol. 12, No. 8, 1021–1038, Aug. 1998.

12. Ling, F., C. F. Wang, and J. M. Jin, "An efficient algorithm for analyzing large-scale microstrip structures using adaptive integral method combined with discrete complex-image method," *IEEE Trans. Antennas Propagat.*, Vol. 48, No. 5, 832–839, May 2000.

13. Medgyesi-Mitschang, L. N. and J. M. Putnam, "Electromagnetic scattering from axially inhomogeneous bodies of revolution," *IEEE Trans. Antennas Propagat.*, Vol. 32, No. 8, 797–806, August 1984.

14. Medgyesi-Mitschang, L. N., J. M. Putnam, and M. B. Gedera, "Generalized method of moments for three-dimensional penetrable scatterers," *J. Opt. Soc. Am. A.*, Vol. 11, No. 4, 1383–1398, April 1994.

15. Li, J. Y., L. W. Li, and Z. Z. Oo, "Electromagnetic scattering by a mixture of conducting and dielectric objects: Analysis using method of moments," accepted by *IEEE Trans. Vehicular Technology*.

16. Poggio, A. J. and E. K. Miller, "Integral equation solution of three dimensional scattering problems," *Computer Techniques for Electromagnetics*, Chap. 4, Permagon, Elmsford, NY, 1973.

17. Chang, Y. and R. F. Harrington, "A surface formulation for characteristic modes of material bodies," *IEEE Trans. Antennas Propagat.*, Vol. 25, No. 6, 789–795, Nov. 1977.

18. Wu, T. K. and L. L. Tsai, "Scattering from arbitrarily-shaped lossy dielectric bodies of revolution," *Radio Sci.*, Vol. 12, No. 5, 709–718, Nov. 1977.

19. Rao, S. M., D. R. Wilton, and A. W. Glisson, "Electromagnetic scattering by surfaces of arbitrary shape," *IEEE Trans. Antennas Propagat.*, Vol. 30, No. 3, 409–418, May 1982.

Wei-Bin Ewe received his B.Eng. degree in electrical engineering (with first class honors) from University Teknologi Malaysia, Malaysia in 2000. He is currently working toward his Ph.D. degree in electrical engineering in the Department of Electrical and Computer Engineering at the National University of Singapore (NUS). His current research interests are in general areas of computational electromagnetics.

Le-Wei Li received the degrees of B.Sc. in Physics, M.Eng.Sc. and Ph.D. in Electrical Engineering from Xuzhou Normal University, Xuzhou, China, in 1984, China Research Institute of Radiowave Propagation (CRIRP), Xinxiang, China, in 1987 and Monash

University, Mel bourne, Australia, in 1992, respectively. In 1992, he worked at La Trobe University (jointly with Monash University), Melbourne, Australia as a Research Fellow. Since 1992, He has been with the Department of Electrical Engineering at the National University of Singapore where he is currently a Professor. Since 1999, he has been also part-timely with High Performance Computation of Engineered Systems (HPCES) Programme of Singapore-MIT Alliance (SMA) as a SMA Fellow. His current research interests include electromagnetic theory, radio wave propagation and scattering in various media, microwave propagation and scattering in tropical environment, and analysis and design of antennas. In these areas, he, as the principal author of a book entitled *Spheroidal Wave Functions in Electromagnetic Theory* by John Wiley in 2001, has published 31 book chapters, over 160 international refereed journal papers, 25 regional refereed journal papers, and over 170 international conference papers. He serves as an Associate Editor of *Journal of Electromagnetic Waves and Applications* and *Radio Science*, an Editorial Board Member of *IEEE Transactions on Microwave Theory and Techniques, Electromagnetics* journal, and an Overseas Editorial Board Member of *Chinese Journal of Radio Science.*

Mook-Seng Leong received the B.Sc. degree in electrical engineering (with first class honors) and the Ph.D. degree in microwave engineering from the University of London, England, in 1968 and 1971, respectively. He is currently a Professor of Electrical Engineering at the National University of Singapore. His main research interests include antenna and waveguide boundary-value problems. Dr. Leong is a member of the MIT-based Electromagnetic Academy and a Fellow of the Institution of Electrical Engineers, London. He received the 1996 Defence Science Organization (DSO) R&D Award from DSO National Laboratories, Singapore in 1996. He is a member of the Editorial Board for Microwave and Optical Technology Letters and Wireless Mobile Communications.